JOURNAL OF PROPULSION AND POWER
Vol. 14, No. 5, September–October 1998

Scaling of Thrust in Self-Field Magnetoplasmadynamic Thrusters

Edgar Choueiri*
Princeton University, Princeton, New Jersey 08544

The magnetoplasmadynamic thruster (MPDT) has recently passed milestones in performance and lifetime that have prompted renewed interest in its unique advantages for energetic space missions. Mission and system studies, as well as ongoing performance characterization, require the use of simple relations for the scaling of performance parameters. The Maecker formula has long played such a role for the thrust of the self-field MPDT. The formula is shown to be too simplistic to account for the trends in measured thrust data that exhibit departures from the model, particularly at low current. We show that at high currents, the departures can be explained by the evolution of the current densities over the electrode surfaces that influence the spatial distribution of the volumetric Lorentz force densities. At low current levels the departures are attributed to the scaling of gasdynamic pressure distributions induced by the pinching components of the volumetric electromagnetic forces. The insight was used to formulate a more accurate empirically based model for the scaling of the thrust of an MPDT.

Nomenclature

a_0 = ion acoustic speed
$\boldsymbol{B}$ = magnetic field
C_T = thrust coefficient
I_{sp} = specific impulse
J = total current
J_{ci} = critical ionization current
$\boldsymbol{j}$ = current density
j_i, j_o = current densities on upstream and downstream faces of anode
$\dot{m}$ = mass flow rate
p = pressure
r = radial coordinate
r_a = anode radius
r_c = cathode radius
r_{ch} = chamber radius
T = thrust
T_e = electron temperature
$\boldsymbol{u}$ = velocity
u_{ci} = critical ionization velocity
u_{ex} = exhaust velocity
z = axial coordinate
$\tilde{\beta}$ = Maxwell stress sensor
γ = specific heat ratio
ε_i = first ionization potential
θ = azimuthal coordinate
μ_0 = permeability of free space
ν = dimensionless mass flow rate
ξ = dimensionless current; self-field MPDT scaling parameter
ρ = density
ϕ = fraction of total current attached at the cathode tip

Subscripts
AIF = anode inner face
AOF = anode outer face
BP = backplate
b = blowing
c = cold thrust component
p = pinching

Received Sept. 2, 1997; revision received May 29, 1998; accepted for publication June 1, 1998.

*Chief Scientist, Electric Propulsion and Plasma Dynamics Laboratory (EPPDyL), Assistant Professor, Applied Physics Group, Mechanical and Aerospace Engineering Department, and Associated Faculty at the Department of Astrophysical Sciences. Senior Member AIAA.

I. Introduction

THE magnetoplasmadynamic thruster (MPDT) is an electromagnetic plasma accelerator intended for spacecraft propulsion. The MPDT, shown schematically in Fig. 1, is essentially a coaxial device in which a high-current discharge ionizes a gas and accelerates it to high exhaust velocities through the action of the Lorentz force produced by the interaction between the current flowing through the plasma and a self-induced or applied magnetic field. The schematic in the figure shows the self-field version with no applied magnetic field. The vectors $\boldsymbol{j}$ and $\boldsymbol{B}$ represent the current density and the induced magnetic field, respectively. References 1–3 give a review of research on MPDT from its inception[4] in 1963 until 1991. In this section we first briefly review the present status of MPDT technology, present a statement of the thrust scaling problem addressed in this paper, and follow with a synopsis of the paper.

A. Status of MPDT Technology

The MPDT has a demonstrated specific impulse (I_{sp}) in the range of 1500–8000 s with thrust efficiencies exceeding 40%.[1] High efficiency (above 30%) is typically reached only at high power levels (above 100 kW)[5] and, consequently, the steady-state version of the MPDT is regarded as a high-power propulsion option. It has the unique capability, among all developed electric thrusters, of processing very high power levels (megawatt level) in a simple, small, and robust device producing thrust densities as high as 10^5 N/m^2. These features have rendered the steady-state MPDT particularly attractive for deep-space energetic (high Δv) missions requiring high thrust levels, such as manned and cargo spacecraft to Mars and the outer planets,[6] as well as for nearer-term orbit-raising missions.[7,8] The present unavailability of high power in space and the cathode erosion rates of the steady-state MPDT (which can be as high as 0.2 μg/C), have, until recently, impeded the evolution of steady-state MPDTs toward flight applications.

A version of the steady-state MPDT, called the lithium Lorentz force accelerator (Li–LFA), which uses a multichannel hollow cathode and lithium for propellant, promises to solve the

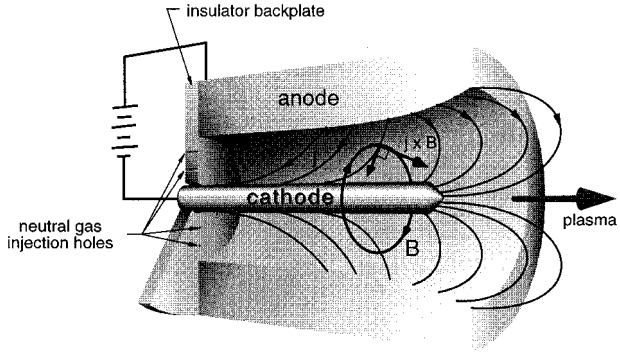

Fig. 1 Schematic of the self-field MPD thruster.

cathode erosion problem while raising the thrust efficiency at moderately high power levels.[9] Recently, a thrust efficiency of 43% at an I_{sp} of 3460 s was measured in Moscow[10] for a low-erosion Li–LFA operating at 130 kW. The thrust-to-power ratio of these devices is typically about 25 N/MW. The extension of the lifetime of such thrusters to above 1000 h has been recently shown to be within reach, with the demonstration of 500 h of practically erosion-free operation of a 50%-efficient Li–LFA at 0.5 MW.[11] Because no other single electric thruster has yet demonstrated the capability of processing that much power (500 kW), producing that much thrust (12.5 N), and operating for that long (500 h) without significant erosion, the Li–LFA is at the forefront of propulsion options for nuclear-powered deep space human exploration and heavy cargo missions to the outer planets.

Ongoing research activities in Moscow,[12] Jet Propulsion Laboratory, and Princeton[13] on the Li–LFA, and in Stuttgart[14] and Pisa[15] on the gas-fed MPDT, aim at further improving the performance and lifetime of the steady-state MPDT, to meet near-future advanced propulsion needs.

To benefit from the advantages of MPD propulsion on today's power-limited spacecraft, the MPDT can be operated in a quasisteady (QS) pulsed mode,[16,17] where flat-top high-current pulses longer than 350 μs are long enough for a steady-state current pattern to dominate the acceleration process [as opposed to the pulsed plasma thruster (PPT), in which an unsteady current sheet is at play]. The QS–MPDT can thus benefit from the high efficiency warranted by the instantaneous high power while drawing low steady-state power from the spacecraft bus. This approach was adopted in the first MPDT to fly as a propulsion system, a 1-kW-class QS–MPDT that operated successfully in 1996 onboard the Japanese Space Flyer Unit.[18]

B. Statement of MPDT Thrust Scaling Problem

It is useful to have a simple analytical model or formula that can readily be used to predict the scaling of the thrust of MPDTs for a wide range of interesting operation parameters, e.g., current, mass flow rate, geometry, and propellant type. Such a formula would be useful for characterizing thruster performance as well as for system and mission analysis. The Maecker equation,[19] described later, is such a formula. However, as we shall see, it can suffer from substantial inaccuracies when applied to real thrusters under many conditions of interest.

The MPDT is considered to be an electromagnetic accelerator in which the acceleration is primarily a result of the action of the Lorentz force. In this paper we will be concerned only with the self-field MPDT,[1] i.e., with no applied magnetic field (from here on, MPDT refers to the self-field version only). The thrust produced by a coaxial self-field electromagnetic plasma accelerator was first treated analytically by Maecker[19] and expounded by Jahn.[20] The resulting expression, often referred to as the Maecker formula, simply states that

$$T = (\mu_0/4\pi)[\ell n(r_a/r_c) + \tfrac{3}{4}]J^2 \tag{1}$$

where J is the current driven between the electrodes. It is convenient for our discussion to define a dimensionless thrust coefficient, C_T, of order unity

$$C_T \equiv (4\pi/\mu_0)(T/J^2) \tag{2}$$

which, for the case of the Maecker formula, is

$$C_T = \ell n(r_a/r_c) + \tfrac{3}{4} \tag{3}$$

Most notable in the Maecker formula is that the thrust coefficient is independent of J, $\dot{m}$, and the type of propellant used.

Although the Maecker formula is derived from an idealized model of the MPDT, it has often been indiscriminately applied to explain the scaling of the thrust of real MPDTs. Not surprisingly, the invariance with J, $\dot{m}$, and the propellant predicted by the formula is most often contradicted by experimental thrust measurements. This is illustrated in Fig. 2, where the measured thrust coefficient of an MPDT (obtained, to a constant, by dividing the measured thrust with the square of the measured current), is plotted vs the measured current for two different argon mass flow rates along with the constant C_T of the Maecker formula.

The argon thrust measurements were made by Gilland[21] using the Princeton benchmark thruster (PBT). The general trends in the figure are typical of data from other thrusters. While the data were obtained with a pulsed thruster, the rectangular pulse duration (1 ms) is long enough for steady-state conditions to be valid[17] for plasmadynamical phenomena, thus allowing the inference of a steady-state thrust.[22,23]

The following features and trends can be noted from the plot:

1) Generally, C_T is dependent on the mass flow rate and current, contrary to the Maecker formula.

2) At high current levels the thrust coefficient does reach a somewhat steady value; however, the Maecker model overpredicts C_T by more than 20%. Even in this high-current range, C_T still exhibits a (weak) dependence on the total current with a weakly pronounced minimum.

3) While at high current levels the measured C_T does become somewhat insensitive to the mass flow rate, the mass flow rate dependence becomes more pronounced as the current is lowered, and eventually goes into a regime where C_T strongly depends on $\dot{m}$.

4) At low current levels the measured C_T rises quickly with decreasing current and can easily reach more than 250% of the Maecker value.

5) The current value at which this transition happens occurs at a lower current when the mass flow rate is decreased.

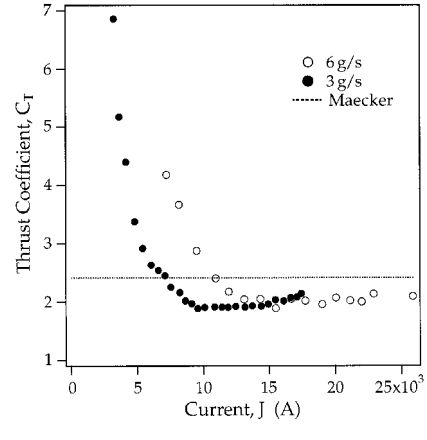

Fig. 2 Comparison of the Maecker thrust coefficient with that measured[21] for the PBT (r_a/r_c = 5.26) with two different argon mass flow rates.

In light of this comparison, it is obvious that the Maecker model is too idealized to account for the thrust scaling of real MPDTs with complex geometries, and that it can become wholly inaccurate when applied at low current levels. In the context of attempting to understand these departures and find a more accurate thrust scaling model, it is convenient to distinguish between two scaling problems corresponding to low and high current operation.

At high current levels, the discrepancy is often reconciled in the literature by substituting for the constant $\frac{3}{4}$ in Eq. (1), a value that causes the model to better fit the data, or by replacing the thrust coefficient, given in (Eq. 3) by $\ell n(r_a/r_c)_{\text{eff}}$, where $(r_a/r_c)_{\text{eff}}$ is an effective value that provides better fit to the formula. These adjustments are often arbitrary, and in both instances C_T remains constant for a given thruster.

It is often assumed that the departure at low current levels must be linked to an increase in the prominence of electrothermal acceleration related to the heating and expansion of the gas. However, from experimental data such as those in Fig. 2, we note that at low current levels C_T scales with J^{-n}, where n is between 3 and 4. This implies that the thrust (proportional to $C_T J^2$) produced by this additional mechanism must scale inversely with J raised to a power greater than 1. This means not only that the fraction of the supposedly electrothermal to electromagnetic thrust must decrease with increasing current (as is intuitive), but also that the magnitude of this nonelectromagnetic additional thrust must (in a certain low-current range) also decrease with increasing current. It is difficult to explain how electrothermal acceleration can be made to decrease with increasing electrical power. This dilemma can be resolved, as will be shown in this paper, by accounting for the role of the electromagnetic pinching forces in regulating the gasdynamic pressure.

C. Synopsis

In Sec. II we discuss the Tikhonov formula,[24] which is an improvement on the Maecker formula. Tikhonov used a simple one-dimensional description of the MPDT to derive a formula for C_T that is not a constant except at high currents. While the poor agreement found can be attributed to the PBT's violation of the model's simple assumptions, the formula does show a J^{-n} dependence for C_T at low currents. In particular, the model shows that n is equal to 4 under the quasi-one-dimensional assumption.

To rigorously distinguish the various sources and dependencies of the MPDT thrust, we proceed in Sec. III with a detailed analytical description, based on first principles, of the thrust of a particular thruster: the PBT. The PBT was selected because of the enormous experimental database accumulated with that configuration, including all of the thrust data used in this paper. Using the results of research carried on at Princeton over the span of two decades, we explore the scaling and dependencies of the thrust and its departure from the simple prescriptions.

By using experimental data with the analytical model, a semiempirical evaluation is carried out for thrust as a function of the current at a fixed argon mass flow rate of 6 g/s. The predicted $T(J)$ dependence of the semiempirical evaluation is compared for the first time with thrust measurements, allowing an interpretation of the departure from the Maecker law in terms of the evolution of the blowing and pinching effects with the current.

In Sec. IV, we combine the insight gained from the previous sections with the notion of a nondimensional similarity parameter that scales various aspects of MPDT behavior. This allows us to formulate a simple semiempirical scaling formula that can be used to predict the thrust scaling as a function of the current, r_a/r_c, mass flow rate, and propellant type. The formula is subsequently tested for both argon and xenon and over a wide range of currents and mass flow rates.

II. Previous Scaling Relations

As mentioned in Sec. I, the Maecker formula is derived for an idealized MPDT and often does not conjugate well with the thrust measurements of real MPDTs with complex geometries. The extent of agreement and departure between theory and experiments were described in Sec. II in the context of Fig. 2. In Sec. III, the sources of these departures will be clarified when we consider the Maecker model as a special case of a more generalized treatment of the real thruster that was used for the measurements. However, before we look at a more complex analysis, it is informative to consider another simple MPDT thrust formula that has been proposed[24,25] (referred to as "Tikhonev"). Unlike the Maecker formula, that of Tikhonov allows for a C_T that does vary with the current.

Tikhonov treats the case of a cylindrical MHD channel flow in the MPDT under the following assumptions: 1) quasi-one-dimensional flow, 2) single fluid, single temperature, 3) isothermal, and 4) high magnetic Reynolds number. By setting the downstream end of the channel to be at the section where the magnetic and thermal pressure become equal, and the upstream end to be at a section immediately behind all the enclosed current, he derives the following simple expression for the thrust coefficient:

$$C_T = [(\gamma + 1)/2] + (\alpha_0^{-2}/2) \tag{4}$$

where α_0 is a dimensionless parameter evaluated at the upstream end of the channel

$$\alpha_0 = \frac{\gamma \mu_0}{8\pi a_0} \frac{J^2}{\dot{m}} \tag{5}$$

a_0 is the ion acoustic speed evaluated at the upstream end. Notably, the expression is independent of r_a/r_c, the propellant ionization potential, and much of the geometrical details of the electrodes. Furthermore, it states that when $J^2/\dot{m}$ becomes high, i.e., $\alpha_0 >> 1$, the thrust coefficient is simply

$$C_T \simeq (\gamma + 1)/2 \tag{6}$$

(which for a monatomic gas, $\gamma = 5/3$, has a value of 1.33).

In Fig. 3 we compare the Tikhonov thrust coefficient with the measured thrust coefficient of the PBT plotted vs the measured current for two different argon mass flow rates. Also shown is the constant Maecker C_T. (The ion acoustic speed, for the Tikhonov C_T, was calculated for 1 eV.) From this figure we find that at high current C_T is underpredicted. It is interesting to note, however, that the Tikhonov model clearly shows the trend of increasing C_T with decreasing current and specifically a scaling of J^{-4} for the thrust coefficient as the current is decreased. Even though the model's agreement with the data is limited (because of the simplistic assumptions that prevent its direct application to the PBT) it does, unlike the Maecker formula, show the general trend of the data.

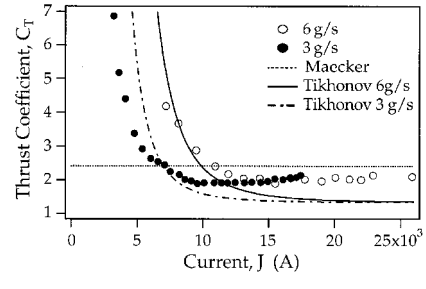

Fig. 3 Comparison of the Tikhonov thrust coefficient with the measured thrust coefficient of the PBT.

III. Detailed Analysis of the Thrust of an MPDT

A. First-Principles Model

It was Rudolph[26] who analytically treated the thrust of the PBT starting from first principles. At the time of that work in 1980, there were no direct thrust measurements available on the PBT. The extensive database available now will allow us to confirm the predicted trends and better understand the differences between measured thrust and the predictions of the simpler models. We will follow the analysis in Ref. 26 and include some effects neglected in that work. These additional effects are essential to explain the departures of the data from the simple models such as the Maecker formula.

Figure 4 shows a schematic of the PBT configuration with a central cathode (10 cm long) and an outer anode (5.1 cm i.r.). The neutral gas is injected from ports in the backplate (left side of the figure), which, like the chamber walls, is an insulator. Also shown in the figure are the cylindrical coordinate system and the boundary (dashed line) of the control volume adopted for the analysis. For the particular thruster used in the thrust experiments we have $r_c = 0.95$ cm, $r_a = 5.1$ cm, $r_{a0} = 9.3$ cm, $r_{ch} = 6.4$ cm, $t_a = 0.95$ cm, and $l_c = 10$ cm.

The control volume denotes the region where electromagnetic, gasdynamic, and viscous shear forces act on the propellant, thus producing a momentum flux. The thrust is equal to the net momentum flux carried away by the propellant flow. The control volume is chosen such that all of its free boundaries are far enough from the thruster to warrant setting the magnetic field there to zero and the pressure equal to the ambient pressure. With these boundary conditions, the only forces that need to be considered are those on the thrust surfaces and inside the control volume. Because we are interested in thrust as the axial component of the force, we can write

$$\int_S \rho u_z(\boldsymbol{u}\cdot \mathrm{d}\boldsymbol{S}) = +\int_V j_r B_\theta \, \mathrm{d}V - \int_S p(\boldsymbol{z}\cdot \mathrm{d}\boldsymbol{S}) \tag{7}$$

where S and V are the surface and volume of the control volume, respectively, and $\boldsymbol{z}$ is the unit vector. The left side of Eq. (7) is the net momentum flux, which is the difference between the thrust and the "cold" thrust T_c resulting from the cold slow gas entering the control volume. We therefore have

$$T = T_c + \int_V j_r B_\theta \, \mathrm{d}V - \int_S p(\boldsymbol{z}\cdot \mathrm{d}\boldsymbol{S}) \tag{8}$$

The second term on the right-hand side (RHS) of Eq. (8) represents the contribution of $j_r B_\theta$, the axial component of the Lorentz force density, which acts to "blow" the plasma out.

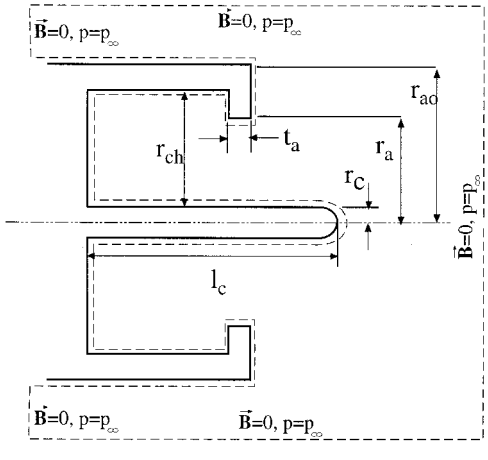

Fig. 4 Control volume used in deriving a thrust equation for the PBT.[26]

This term will be referred to as T_b, the blowing contribution to thrust. The radial component of the Lorentz force density, $j_z B_\theta$, acts to pinch the plasma and contributes to axial thrust through the unbalanced effect of the gasdynamic pressure on some surfaces of the accelerator. Consequently, the second integral on the RHS is an integral of the gasdynamic pressure and represents the "pinching" contribution of the Lorentz force to the axial thrust and is termed T_p. This integral contains, implicitly, the effects of $j_z B_\theta$.

The cold gas contribution T_c is typically much smaller than the total thrust and will be neglected in this analysis. Also neglected in Eq. (8) are viscous effects. In SI units, a typical plasma viscosity of 10^{-5}, a velocity of 10^4, and a boundary-layer thickness of about 1 mm yield a viscous force of 10^{-2} N/cm^2.[27] For a thruster whose total wall surface area is on the order of 100 cm^2, the viscous force is negligible compared to the thrust of the PBT, which is typically on the order of 100 N.

1. Blowing Contributions

The evaluation of T_b through volume integration, as prescribed by the second term on the RHS of Eq. (8), requires knowledge of the details of the current distribution inside the chamber. However, by using the concept of the magnetic stress tensor, the volume integral can be replaced by a far more useful surface integral.[20,26] By definition, the Maxwell stress sensor, $\tilde{\beta}$, satisfies the following equation:

$$\nabla\cdot\tilde{\boldsymbol{\beta}} = \boldsymbol{j}\times\boldsymbol{\beta} \tag{9}$$

which, when combined with Maxwell's equations for the divergence and curl of the magnetic field, yields

$$\nabla\cdot\tilde{\boldsymbol{\beta}} = \frac{(\nabla\times\boldsymbol{B})\times\boldsymbol{B}}{\mu_0} \tag{10}$$

This equation allows us to relate the volume integral of the Lorentz body force density to a surface integral through the divergence theorem

$$T_b = \int_V j_r B_\theta \, \mathrm{d}V = \int_V (\nabla\cdot\tilde{\boldsymbol{\beta}})_z \, \mathrm{d}V = \int_S (\tilde{\boldsymbol{\beta}}\cdot \mathrm{d}\boldsymbol{S})_z \tag{11}$$

For a coaxial self-field MPDT with a symmetric discharge, the magnetic field has only an azimuthal component and the magnetic stress tensor takes the form

$$\tilde{\beta} = \frac{1}{\mu_0}\begin{bmatrix} -\dfrac{B_\theta^2}{2} & 0 & 0 \\ 0 & \dfrac{B_\theta^2}{2r^2} & 0 \\ 0 & 0 & -\dfrac{B_\theta^2}{2} \end{bmatrix} \tag{12}$$

The only areas of the control volume surface shown in Fig. 4 that contribute to the surface integral in Eq. (11) are the four that are perpendicular to the thrust axis and over which the magnetic field is finite. These are the backplate, the anode outer (downstream) surface, the anode inner (upstream) surface, and the tip of the cathode. The anode lip, which in reality is rounded, will be approximated by a flat surface as shown in Fig. 4, where all of the physical dimensions of the PBT that are needed for the evaluation of the integral are defined.

The analytical thrust model shown next differs from that obtained by Rudolph,[26] in that it does not contain the effects of current attachments on the outside cylindrical part of the thruster and it assumes a nonuniform gasdynamic pressure radial profile on the backplate. The pressure radial profile affects

only the pinching contribution and, as will be seen later, is essential to explain the departures from the Maecker model at low currents.

The resulting contributions of the four surfaces to the blowing component T_b are quoted next. Details of the integration can be found in Ref. 26.

a. Backplate blowing contribution. For the backplate we have

$$(T_{em})_{BP} = \left[\int_S p(\tilde{\boldsymbol{\beta}}\cdot \mathrm{d}\boldsymbol{S})_z\right]_{BP} = \int_{r_c}^{r_{ch}} \frac{B_\theta^2}{2\mu_0} 2\pi r\, \mathrm{d}r \tag{13}$$

where Ampere's law is used to get the value of B_θ at the backplate

$$B_\theta = \mu_0 J/2\pi r \tag{14}$$

because J is all downstream of the backplate. The integration yields an expression for the backplate contribution $(T_{em})_{BP}$

$$(T_b)_{BP} = \frac{\mu_0}{4\pi}\,\ell n\,\frac{r_{ch}}{r_c}\,J^2 \tag{15}$$

b. Anode inner face blowing contribution. The evaluation of B_θ from Eq. (14) for the anode inner face requires knowledge of the enclosed current, J_{enc} at the various radii along that surface. This can be found in terms of j_i on the anode inner face through

$$J_{enc}(r) = J - \int_r^{r_{ch}} j_i\, \mathrm{d}S \tag{16}$$

because this current density acts to diminish the enclosed current from its maximum value J at the corner between the anode inner face and the chamber wall. We shall assume that this current density stays, to a first order, uniform, and is given by experiments. Under this assumption

$$J_{enc}(r) = J - j_i\pi(r_{ch}^2 - r^2) \tag{17}$$

and the integration yields the following expression for the anode inner face contribution $(T_{em})_{AIF}$:

$$(T_b)_{AIF} = -\frac{\mu_0}{4\pi}\left[(J^2 - 2\pi r_{ch}^2 j_i J + \pi^2 r_{ch}^4 j_i^2)\,\ell n\,\frac{r_{ch}}{r_a} + (\pi J j_i - \pi^2 r_{ch}^2 j_i^2)(r_{ch}^2 - r_a^2) + \frac{\pi^2 j_i^2}{4}(r_{ch}^4 - r_a^4)\right] \tag{18}$$

c. Anode outer face blowing contribution. In similar fashion, an expression for the enclosed current J_{enc} as a function of r along the outer face of the anode can be written, again assuming that the current density there j_0 is uniform and that no current attaches on the outer cylindrical part of the thruster (which was insulated for the thruster used in the thrust experiments)

$$J_{enc} = \pi j_0(r_{a0}^2 - r^2) \tag{19}$$

This leads to

$$(T_b)_{AOF} = \frac{\mu_0}{4\pi}\left[\pi^2 r_{a0}^4 j_0^2\,\ell n\,\frac{r_{a0}}{r_a} - \pi^2 r_{a0}^2 j_0^2(r_{a0}^2 - r_a^2) + \frac{\pi^2 j_0^2}{4}(r_{a0}^4 - r_a^4)\right] \tag{20}$$

where j_0 is the current density on the outer face of the anode.

d. Cathode tip blowing contribution

$$(T_b)_{CT} = \frac{\mu_0 \phi^2 J^2}{4\pi}\left(\frac{3}{2} - 2\,\ell n\,2\right) \tag{21}$$

where the cathode tip is taken to be hemispherical.

The final expression for T_b is obtained by summing the four contributions given by Eqs. (15), (18), (20), and (21).

2. Pinching Contributions

To evaluate the surface integral of the gasdynamic pressure in Eq. (8), we consider the radial momentum balance

$$\rho u_r \frac{\partial u_r}{\partial r} = -\frac{\partial p}{\partial r} - j_z B_\theta \tag{22}$$

where the term $\rho u_z \partial u_r/\partial z$ does not appear because u_z is zero on the solid surfaces over which the integral will be evaluated (backplate, inner and outer anode faces, and the cathode tip). This yields the following expression for $p(r, z)$ along the surfaces of the control volume:

$$p(r, z) = \int_r^{r_0} \rho u_r \frac{\partial u_r}{\partial r}\,\mathrm{d}r + \int_r^{r_0} \frac{B_\theta}{\mu_0 r}\frac{\partial r B_\theta}{\partial r}\,\mathrm{d}r + p(r_0, z) \tag{23}$$

where Maxwell's $\nabla \times \boldsymbol{B}$ equation was used to eliminate j_z. The last term, $p(r_0, z)$, is the integration constant taken as the gasdynamic pressure at an arbitrary radius r_0.

The magnitude of the integrand in the first integral can be estimated to be on the order of 10^4 N/m^3, using an upper limit on the plasma density 10^{22} m^{-3} (which gives $\rho = 6.6 \times 10^{-4}$ kg/m^3 for argon), velocities of 10^4 m/s, and a characteristic length of 5 cm. This magnitude is typically much lower than that of the radial pinching force density as estimated from measurements by Rudolph.[26] Consequently, Rudolph assumes the radial flow term to be negligible in his analysis. We shall see that to explain the rise in C_T at lower currents the radial flow term should not be neglected, at least for the case of the backplate pinching contribution to thrust.

a. Backplate pinching contribution. The pinching contribution of the backplate part of the control volume presents an interesting singularity: the second integral in Eq. (23) vanishes because all of the current is downstream of the backplate and rB_θ is a constant there. This implies that the pressure gradient on that surface is balanced by the radial flow term only. This gives a thrust contribution of

$$(T_p)_{BP} = \left[-\int_S p(\boldsymbol{z}\cdot \mathrm{d}\boldsymbol{S})\right] = p(r_{ch}, z_0)\pi(r_{ch}^2 - r_c^2) + \int_{r_c}^{r_{ch}} 0\pi r\left(\int_r^{r_{ch}} \rho u_r \frac{\partial u_r}{\partial r}\,\mathrm{d}r\right)\mathrm{d}r \tag{24}$$

where z_0 refers to the axial position of the backplate. The pressure $p(r_{ch}, z_0)$ was measured at the backplate by Cory,[27] and we will use his measurements in the calculations shown next. We lack, however, an experimental characterization that would allow us to estimate the radial flow term in Eq. (24). If this flow term is neglected, as was done by Rudolph,[26] the pressure profile is flat and the thrust contribution is a constant given by $p(r_{ch}, z_0)\pi(r_{ch}^2 - r_c^2)$. A finite (nonuniform) radial velocity profile, on the other hand, would induce a pressure radial profile at that surface that is peaked at the cathode. Consequently, a better approximation than a flat profile would be a parabolic one centered at the cathode and modeled as

$$p(r, z_0) = b - ar^2 \tag{25}$$

where

$$a = \frac{p(r_c) - p(r_{ch})}{r_{ch}^2 - r_c^2}, \qquad b = p(r_c) + \frac{p(r_c) - p(r_{ch})}{r_{ch}^2 - r_c^2} r_c^2 \quad (26)$$

and where, for the case of the backplate, the pressures are those at $z = z_0$. After integration, this yields the following thrust contribution:

$$(T_p)_{BP} = b\pi(r_{ch}^2 - r_c^2) - \frac{a\pi}{2}(r_{ch}^4 - r_c^4) \quad (27)$$

While the measurements of Cory[27] will be used for $p(r_{ch}, z_0)$, the unknown term $p(r_c, z_0)$ becomes the only free parameter of the model. The value for $p(r_c, z_0)$ will be inferred from the thrust data as will be shown later. Rudolph's approximation of neglecting the radial flow term is equivalent to setting $p(r_c, z_0)$ equal to $p(r_{ch}, z_0)$. This would lead to an underestimate of the pinching contribution to thrust and cannot account for the rise of C_T with decreasing current, as will be shown in the evaluation at the end of this section.

b. Anode inner face pinching contribution. Downstream of the backplate end of the control volume, the second integral in Eq. (23) quickly dominates the radial flow term and, consequently, the pressure profile may be assumed to be induced mainly by the Lorentz term. Using the same assumptions as for the blowing contribution in Eq. (18), the integration yields[26]

$$(T_p)_{AIF} = \frac{\mu_0}{4\pi}\left[(j_i^2\pi^2 r_{ch}^4 + j_i^2\pi^2 r_{ch}^2 r_a^2 - 2Jj\pi r_{ch}^2)\frac{r_{ch}^2 - r_a^2}{2r_{ch}^2} - (2r_a^2 j_i^2\pi^2 r_{ch}^2 - 2Jj_i\pi r_a^2)\,\ell n\frac{r_a}{r_c}\right] - \pi(r_{ch}^2 - r_a^2)p(r_{ch}, z_0) \quad (28)$$

We have again assumed the pressure constant to be $p(r_{ch}, z_0)$.

c. Anode outer face pinching contribution. The plasma density on the 200 cm^2 anode of the PBT does not exceed an upper limit[27] of 10^{20} m^{-3}, so that even for a temperature as high as 5 eV the pressure force will be less than 2 N and can be neglected.

d. Cathode tip pinching contribution. This contribution is also quite small because ϕ is typically on the order of 10%. Following the prescriptions used earlier to get the blowing contribution at the cathode tip, and neglecting the radial flow term, the integration of Eq. (25) yields[26]

$$[T_p]_{CT} = \frac{\mu_0}{4\pi}\frac{\phi^2 J^2}{12} + p(r_c, z_{tip})\pi r_c^2 \quad (29)$$

where $p(r_c, z_{tip})$ is the pressure at the cathode tip available from experiments.

The total thrust is the total sum of the blowing contribution expressed in Eqs. (15), (18), (20), and (21) and the pinching contributions expressed in Eqs. (27), (28), and (29).

B. Comparison to the Maecker Formula

As previously mentioned, the total thrust model presented earlier differs from that obtained by Rudolph[26] in that it does not contain the effects of current attachments on the outside cylindrical part of the thruster and that it assumes a nonuniform pressure radial profile on the backplate.

To see the difference from the Maecker formula as presented by Jahn,[20] we show in Fig. 5 the control volume used to derive that formula following the Maxwell stress tensor approach. This choice of control volume is equivalent to considering the thruster as an infinite cylinder without a backplate.

The differences between the resulting simple formula and the detailed model derived in the previous text can be attributed to the following:

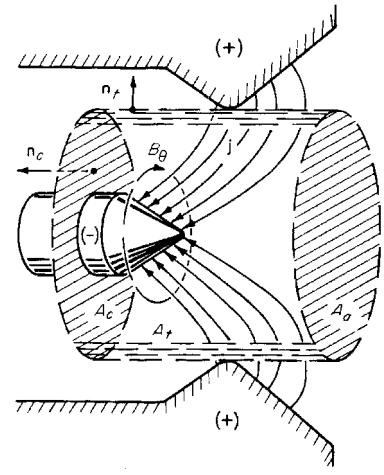

Fig. 5 Control volume used in deriving the Maecker formula.[20]

1) The Maecker formula does not include effects of current attachment on surfaces that are not parallel to the thruster axis (note the simple cylindrical control volume used in Fig. 5).

2) While the Maecker formula assumes that all the current attaches uniformly at the cathode tip, the previous treatment allows for a more diffusive current attachment over the cathode length with a fraction ϕJ attaching at the tip.

3) In the Maecker formula the blowing component contributes a term of $(\ell n\, r_a/r_c + 1/4)$ to C_T, assuming uniform current density on the cathode surface, and a constant of 1/2 from the pinching pressure on the cathode tip, giving a constant equal to 3/4. It does not include the effects of pinching pressure on the backplate of the thruster.

For the PBT at high currents, the blowing contribution at the backplate dominates, while the terms for blowing and pinching at the cathode tip, even if ϕ is near unity, contribute a thrust coefficient below 0.2, which is far lower than the corresponding 3/4 term in the Maecker formula. We shall see later that at high currents, the pinching contribution at the backplate is not high enough to exceed the C_T of the Maecker formula. At low currents, however, the pinching pressure effects on the backplate cause an enhancement in C_T above the Maecker value.

C. Semiempirical Evaluation

So far, the thrust model, represented by Eqs. (15), (18), (20), (21), (27), and (28) is purely analytical and derived from first principles. However, it cannot inform us as to how C_T varies with the current because we lack a formulation of how the following parameters vary with J:

$$j_i, j_o, \phi, p(r_c, z_{tip}), p(r_{ch}, z_0) \quad (30)$$

A prescription of this sort can be obtained from experimental measurements of current distribution along the electrodes as a function of J and pressure measurements. The use of an experimental prescription of these parameters will render the model semiempirical and applicable only for the conditions, e.g., $\dot{m}$, propellant type, under which the thruster, used for the experiments, was operated. Such a semiempirical evaluation of the model is useful in showing the general thrust scaling trends and will be of guidance to our efforts to formulate a more generalized thrust scaling relation in Sec. IV.

Using the current density measurements reported in Refs. 26, 28, and 29, the evolution of j_i and j_o (along the anode inner and outer faces) with the total current J was deduced to have the following general trend. Below a first transition current J_{t1}, the current attaches entirely to the inner face of the anode. Above J_{t1}, but below another transition current J_{t2}, j_i on the inner face stays constant while j_{lip} on the anode lip becomes finite and increases with increasing J until J_{t2} is reached. Above

this limit any additional increase in J is attached at the outside face of the anode while both j_i and j_{lip} stay constant. By requiring that $J = j_i S_i + j_{lip} S_{lip} + j_o S_0$ (where S is the area of each surface), and assuming the current densities to be uniform over these areas, we can write

$$J \leq J_{t1}: j_i = \frac{J}{S_i}, \qquad j_{lip} = 0, \qquad j_o = 0$$

$$J_{t1} \leq J \leq J_{t2}: j_i = \frac{J_{t1}}{S_i}, \qquad j_{lip} = \frac{J - J_{t_1}}{S_{lip}}, \qquad j_o = 0 \tag{31}$$

$$J_{t2} < J: j_i = \frac{J_{t1}}{S_i}, \qquad j_{lip} = \frac{J_{t2} - J_{t_1}}{S_{lip}}, \qquad j_o = \frac{J - J_{t2}}{S_0}$$

For the PBT operating with 6 g/s of argon, we can deduce from Ref. 26 that $J_{t1} = 3.7$ kA and $J_{t2} = 14$ kA.

The dependence of $p(r_{ch}, z_0)$ on the current was measured by Cory[27] and is given by

$$p(r_{ch}, z_0) = 6.5 \times 10^{-4} J^{1.5} \quad \text{N/m}^2 \tag{32}$$

for 6 g/s of argon. Finally, from current density measurements and momentum balance considerations,[26] we have

$$p(r_c, z_{tip}) = 0.263J \quad \text{N/m}^2 \tag{33}$$

and ϕ is essentially constant at 0.2.

With these empirical specifications all of the components of thrust can be calculated with the exception of $(T_p)_{BP}$, which requires knowledge of the dependence of $p(r_c, z_0)$ on J. Consequently, we calculated all of the other components of thrust and subtracted their sum from the measured (total) thrust data at 6 g/s. The remaining contribution represents the pinching contribution at the backplate end of the control volume. Figure 6 shows the evolution of $p(r_c, z_0)$ vs J that is required for Eq. (27) to fit the backplate pinching contribution inferred from the data. It can be noted that as the current is increased beyond about 14 kA, the pressure on that boundary at the cathode radius becomes essentially equal to the pressure at a radius r_{ch} and is given by Cory's empirical formula. This means that, above this current, the pressure radial profile is flat, as assumed by Rudolph.[26] However, below that current level, a substantial difference between the pressure at r_c and that at r_{ch} is required to explain the data. The pressure radial profiles corresponding to the curves in Fig. 6 are shown in Fig. 7 for four different current levels.

Figure 8 shows the contributions of the various blowing and pinching components to C_T along with their total sum. Because of the lack of experimental data below 5 kA, all extrapolations to lower currents are unreliable and, consequently, the corresponding portions of the curves in that figure are meaningless. It is clear from Fig. 8 that at high current levels, the main contribution to the thrust is from the blowing component at

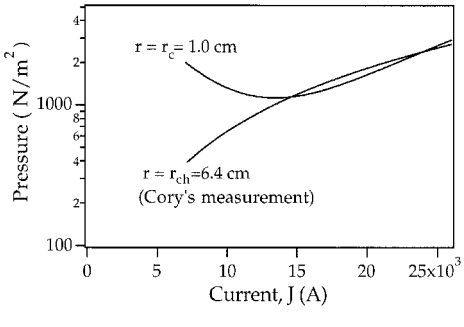

Fig. 6 Evolution of the gasdynamic pressure on the backplate at the cathode ($r = r_c$) inferred from the measured data. Also shown is the presssure at a radius ($r = r_c h$) as measured by Cory[27] [cf. empirical formula in Eq. (32)]

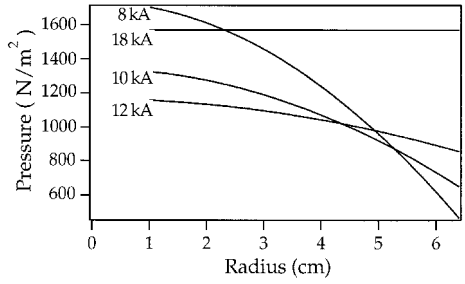

Fig. 7 Radial profiles of the pressure at the backplate corresponding to the curves shown in Fig. 6 for four different current levels.

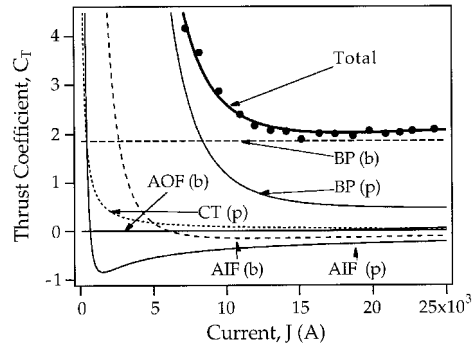

Fig. 8 Contributions of the various blowing and pinching components to C_T, along with their total sum for the PBT operated with 6 g/s of argon. Also shown are the measured data. Values corresponding to current levels below 5 kA are not reliable.

the backplate with a small contribution from the pinching component, which, from Fig. 6, can be seen to be fully accounted for by Cory's pressure measurements at $r = r_{ch}$. As the current is decreased, the pressure at the cathode end of the backplate must increase above its value at higher radii to account for the rise in C_T.

The rise in C_T at lower current, according to this picture, can be explained not by the scaling of thrust caused by the expansion of an ohmically heated gas, but rather by the scaling of gasdynamic pressure distributions induced by the pinching effect of the volumetric Lorentz force densities.

IV. Formulation of a Simple Scaling Relation

It is desirable to have a simple, albeit semiempirical, $C_T(J)$ formula that would be applicable over a wide range of parameters and would be valid for other mass flow rates and propellants then 6 g/s of argon. To rigorously derive a $C_T(J)$ formula from the preceding analysis would require explicit expressions for all of the thrust contributions in the preceding thrust model as functions of the total current. This is not possible because we lack a model for the dependence of the pressure fields on J. Such a model is beyond the scope of this study. Therefore, we will invoke some of the dependencies found earlier, along with phenomenological arguments, to formulate a semiempirical $C_T(J)$ model of wider applicability. Central to this formulation is the dimensionless current based on the critical ionization velocity.

A. Critical Ionization Velocity and Dimensionless Current ξ

Numerous experiments on the MPDT have shown that the following dimensionless parameter:

$$\xi = J \Big/ \left[\dot{m}^{1/2} \left(\frac{2\varepsilon_i}{m_a} \right)^{1/4} \Big/ \left(\frac{\mu_0}{4\pi} \ell n \frac{r_a}{r_c} \right)^{1/2} \right] \tag{34}$$

(where m_a and ε_i are the mass and the first ionization potential of the neutral atom, respectively) scales various aspects of MPDT behavior such as voltage,[30] thrust,[31] erosion,[32] discharge symmetry,[33] and anode drop.[34] The first scaling relations for MPDT characteristics (voltage and thrust) based on this parameter were derived in 1987.[30] The present section presents, in the light of the preceding results, a refinement of the ξ-based thrust model presented in Refs. 30 and 31.

A physical interpretation for scaling with ξ can be made as follows. In the MPDT, ionization is a significant energy sink whose scaling, under nominal operation of the thruster, is strongly tied to the magnitude of the energy in the acceleration (useful) sink. [The strong tie between these two sinks is suspected to be related to the role of plasma instabilities in controlling and enhancing ionization. (Evidence on the role of plasma instabilities in MPDT ionization was presented in Refs. 35 and 36.) Because instabilities in MPDTs are of the current-driven type,[37,38] and because acceleration in the MPDT is also current-driven, both sinks share the same source, namely the current.] A nominal regime for MPDT operation can thus be defined in terms of this equipartition of energy (or power) sinks that can be stated, in terms of power, as

$$\tfrac{1}{2} T u_{ex} = \dot{m}(\varepsilon_i/M) \tag{35}$$

which, by definition, only holds near the nominal operation point. The velocity u_{ex} in this expression is that of the plasma exhaust. Because $T = (\mu_0/4\pi)C_T J^2$, the preceding relation gives

$$(\mu_0/4\pi)C_T J^2 u_{ex} = \dot{m} u_{ci}^2 \tag{36}$$

where u_{ci} is defined as

$$u_{ci} \equiv (2\varepsilon_i/m_a)^{1/2} \tag{37}$$

and is generally known as the critical ionization velocity. For xenon, argon, and lithium, u_{ci} is 4.22, 8.72, and 12.24 km/s, respectively.

We define "nominal operation" to be that for a thruster current that produces an exhaust velocity equal to the critical ionization velocity. That current is termed J_{ci}. From the preceding equation we have

$$J_{ci} = \left[\frac{\dot{m} u_{ci}}{(\mu_0/4\pi)C_T}\right]^{1/2} \tag{38}$$

This characteristic current is used to nondimensionalize the thruster current giving us the dimensionless parameter ξ defined as

$$\xi \equiv J/J_{ci} \tag{39}$$

which is written more explicitly in Eq. (34), where C_T was taken, to a first order, to be $\ell n(r_a/r_c)$. {For ξ near 1, a better approximation for C_T, as will be seen later, is $\ell n[(r_a/r_c) + 1]$}.

The parameter ξ can be thought of as a similarity parameter in the sense that two thrusters operating at the same value of ξ are expected to exhibit some similar characteristics. Because this similarity is borne out by numerous experiments, we shall adopt it axiomatically in our formulation of a thrust scaling relation and verify its applicability by testing the resulting scaling formula with experimental data over a wide range of parameters.

It is interesting to contrast the dimensionless scaling parameter ξ with the dimensionless parameter α_0 in the Tikhonov formula. The former describes the relative importance of the electromagnetic acceleration energy (power) sink to that of ionization, whereas the latter uses the thermal energy as a reference. The two are related by

$$\xi^2 = c\alpha_0 \tag{40}$$

where c is given by

$$c = \gamma(kT_e/\varepsilon_i)^{1/2}\, \ell n(r_a/r_c) \tag{41}$$

which is typically of order unity.

B. Formulation of a Thrust Scaling Relation

It is clear from Fig. 8 that C_T, at low current levels, scales with J^{-n} and that this dependence can be mostly attributed to the pinching contribution at the backplate. However, because of the lack of explicit expressions for the dependence of the pressure terms in Eq. (26) on the total current, we rely on a data fit of the C_T vs J data to find that n is about 4. This is further upheld by the $C_T \propto J^{-4}$ scaling in the Tikhonov formula, Eq. (4). Therefore, assuming that $C_T \propto J^{-4}$ at low currents and because $J \propto \xi$, we expect the following scaling for small values of ξ:

$$C_T \sim \xi^{-4} \quad (\text{for } \xi < 1) \tag{42}$$

At high current levels ($\xi > 1$), we know from the preceding discussions that C_T scales weakly with the current but is not constant as in the Maecker formula. This is a result of both the dominance of the backplate blowing contribution and the finiteness of all the other terms, which provide the dependence on the current. This dependence is too complex to model as it relates to how the current densities distribute over the electrodes and how that distribution evolves with changing current. It would be much more useful to have a less entangled, albeit empirical, characterization of the scaling of this effect. Fortunately, such a study does exist in the form of an experimental investigation carried by Kaplan,[29] who found that the scaling of the thrust coefficient at high current levels is such that e^{C_T} vs $J^2/\dot{m}$ can be represented by a line whose intercept is very close to the physical value of r_a/r_c. This is shown in Fig. 9, where measurements of the quantity e^{C_T} are plotted vs $J^2/\dot{m}$ for various conditions and with two geometrically similar but different sized PBTs. If only the high-current ($J^2/\dot{m}$) data points on that plot are used for the fit, it can be seen that the intercept of the line is very nearly the value of r_a/r_c, which for that thruster is 5.26.

Based on these considerations and the fact that $J^2/\dot{m}$ scales as ξ^2, we expect the following scaling for the thrust coefficient at high values of ξ

$$C_T \sim \ell n[(r_a/r_c) + \xi^2] \quad (\text{for } \xi > 1) \tag{43}$$

In light of all of the preceding information we can formulate a scaling model that is a combination of Eqs. (42) and (43) in the form of

$$C_T = (\nu/\xi^4) + \ell n[(r_a/r_c) + \xi^2] \tag{44}$$

where ν is a dimensionless mass flow rate that corrects for mass flow rate effects

$$\nu \equiv \dot{m}/\dot{m}^* \tag{45}$$

and where $\dot{m}^*$ is a reference mass flow rate presumed to be a constant and is obtained empirically from the data. Using the expression

$$C_T = (\dot{m}/\dot{m}^*/\xi^4) + \ell n[(r_a/r_c) + \xi^2] \tag{46}$$

with the 6 g/s argon data, yielded

$$\dot{m}^* = 66 \quad \text{g/s} \tag{47}$$

In the narrow sense of applying to data at three mass flow rates of both argon and xenon as well as for two similar thrust-

ers with different length scales, this value for $\dot{m}^*$ is universal as shown by the comparison of the model to these data.

The plot in Fig. 10 is a comparison of the model to the thrust measurements at three mass flow rates of argon, showing that the trends in the data are well accounted for. To test the model's accounting for propellant effects, it is compared in Fig. (11) to both argon and xenon data taken with the same thruster at the same mass flow rate. The agreement was far worse for attempts to model hydrogen data. This could be partly related to the fact that the critical ionization velocity of hydrogen is both very high and ill-defined (diatomic molecule).

Finally, it is important to note that the length scale invariance implicit in the model is borne out by the fact that the 6 g/s argon data in Fig. 10 were obtained with the full-scale PBT, whereas the other data on that plot were obtained with a half-scale PBT[21] (same r_a/r_c).

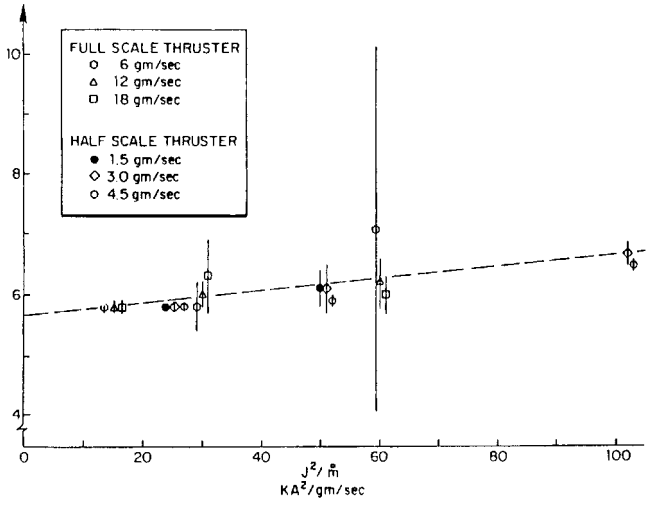

Fig. 9 Scaling of e^{G_T} with $J^2/\dot{m}$, from Ref. 29.

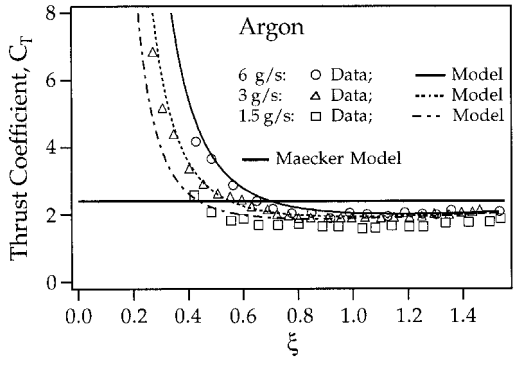

Fig. 10 Comparison of the scaling formula in Eq. (46) with argon thrust measurements for three mass flow rates.

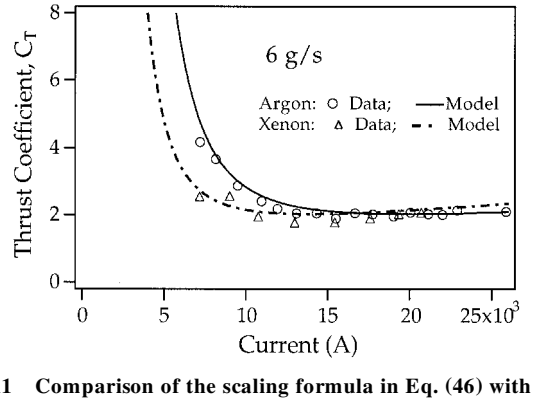

Fig. 11 Comparison of the scaling formula in Eq. (46) with measurements for argon and xenon at a fixed mixed flow rate.

V. Summary

The scaling of thrust in MPD thrusters is shown to depart from the simple prescription of the Maecker formula, which states that the thrust coefficient $C_T = (4\pi/\mu_0)T/J^2$ is constant. The departures at both low and high current levels are clarified by studying the scaling of the various thrust components as a function of current. At high currents, the analysis shows how the particular geometry of a real thruster can yield finite corrections to the simple Maecker model. At low currents, the formula is wholly inadequate in describing the data, with measured thrust coefficients reaching values up to 250% of those prescribed by the formula. It is shown that, in some real thrusters, such as the one used for this study, these departures can be explained not by the scaling of thrust caused by the expansion of an ohmically heated gas, but rather by the scaling of gasdynamic pressure distributions induced by the pinching components of the volumetric electromagnetic forces. The insight was used to formulate a simple but accurate scaling formula that quantitatively describes the trends in an extensive database of measured thrust.

Acknowledgment

This research was supported by NASA–JPL's program on advanced propulsion.

References

[1]Nerheim, V. M., and Kelly, A. J., "A Critical Review of the Magnetoplasmadynamic (MPD) Thrustor for Space Applications," NASA–JPL, TR 32-1196, Pasadena, CA, 1968.

[2]Sovey, J. S., and Mantenieks M. A., "Performance and Lifetime Assessment of MPD Arc Thruster Technology," AIAA Paper 88-3211, July 1988.

[3]Myers, R. M., Mantenieks, M. A., and LaPointe, M. R., "MPD Thruster Technology," AIAA Paper 91-3568, Aug. 1991.

[4]Ducati, A. C., Giannini, G. M., and Muehlberger, E., "Experimental Results in High Specific Impulse Thermoionic Acceleration," *AIAA Journal*, Vol. 2, No. 8, 1964, pp. 1452–1454.

[5]Petrosov, V. A., Safonov, I. B., Utkin, Y. A., and Shutov, V. N., "Investigation of Alkali Metal MPD Thrusters," 24th International Electric Propulsion Conference, IEPC Paper 95-104, Oct. 1995.

[6]Frisbee, R. H., and Hoffman, N. J., "SP-100 Nuclear Electric Propulsion for Mars Cargo Missions," AIAA Paper 96-3173, July 1996.

[7]Polk, J. E., Frisbee, R., Krauthamer, S., Tikhonov, V., Semenikhin, S., and Kim, V., "Technology Requirements for High Power Lithium Lorentz Force Accelerators," *Proceedings of the Space Technology and Applications International Forum*, AIP 387, Pt. 3, American Inst. of Physics, New York, 1997, pp. 1505–1513.

[8]Choueiri, E. Y., Kelly, A. J., and Jahn, R. G., "Mass Savings Domain of Plasma Propulsion for LEO to GEO Transfer," *Journal of Spacecraft and Rockets*, Vol. 30, No. 6, 1993, pp. 749–754.

[9]Polk, J. E., and Pivirotto, T. J., "Alkali Metal Propellants for MPD Thrusters," AIAA Paper 91-3572, June 1991.

[10]Kim, V., Tikhonov, V., and Semenikhin S., "Fourth Quarterly (Final) Report to NASA-JPL: 100–150 kW Lithium Thruster Research," Moscow Aviation Inst., NASW-4851, Moscow, Russia, April 1997.

[11]Ageyev, V. P., and Ostrovsky, V. G., "High-Current Stationary Plasma Accelerator of High Power," 23rd International Electric Propulsion Conference, IEPC Paper 93-117, Sept. 1993.

[12]Tikhonov, V., Semenikihin, S., Brophy, J. R., and Polk, J. E., "The Experimental Performance of the 100 kW Lithium MPD Thruster with External Magnetic Field," 24th International Electric Propulsion Conference, IEPC Paper 95-105, Sept. 1995.

[13]Choueiri, E. Y., Chiravalle, V. P., Miller, G. E., Jahn, R. G., Anderson, W., and Bland, J., "Lorentz Force Accelerator with an Open-Ended Lithium Heat Pipe," AIAA Paper 96-2737, July 1996.

[14]Merke, W. D., Auweter-Kurtz, M., Habiger, H., Kurtz, H., and Schrade, H. O., "Nozzle Type MPD Thruster Experimental Investigations," AIAA Paper 88-028, Sept. 1988.

[15]Paganucci, F., Rossetti, P., and Andrenucci, M., "Current Emission Regimes in an Artificially Heated Cathode of an MPD Thruster,"

AIAA Paper 96-2705, July 1996.
[16]Ashby, D. E. T. F., Liebing, L., Larson, A. V., and Gooding, T. J., "Quasi-Steady-State Plasma Acceleration," *AIAA Journal*, Vol. 4, No. 5, 1966, pp. 831–835.
[17]Clark, K. E., and Jahn, R. G., "Quasi-Steady Plasma Acceleration," *AIAA Journal*, Vol. 8, No. 2, 1970, pp. 216–220.
[18]Toki, K., Shimuzu, Y., and Kuriki, K., "Electric Propulsion Experiment (EPEX) of a Repetitively Pulsed MPD Thruster System Onboard Space Flyer Unit (SFU)," 25th International Electric Propulsion Conference, IEPC Paper 97-120, Aug. 1997.
[19]Maecker, H., "Plasma Jets in Arcs in a Process of Self-induced Magnetic Compression," *Zeitschrift für Physik*, Vol. 141, No. 1, 1955, pp. 198–216.
[20]Jahn, R. G., *Physics of Electric Propulsion*, McGraw–Hill, New York, 1968.
[21]Gilland, J. H., "The Effect of Geometrical Scale upon MPD Thruster Behavior," M.S. Thesis, Princeton Univ., Princeton, NJ, 1988.
[22]Burton, R. L., Clark, K. E., and Jahn, R. G., "Measured Performance of a Multi-Megawatt MPD Thruster," *Journal of Spacecraft and Rockets*, Vol. 20, No. 3, 1983, pp. 299–304.
[23]Cubbin, E. A., Ziemer, J., Choueiri, E. Y., and Jahn, R. G., "Laser Interferometric Measurements of Impulsive Thrust," *Review of Scientific Instruments*, Vol. 68, No. 6, 1997, pp. 2339–2346.
[24]Tikhonov, V. B., Semenihin, S. A., Alexandrov, V. A., Dyakonov, G. A., and Popov, G. A., "Research on Plasma Acceleration Processes in Self-Field and Applied Magnetic Field Thrusters," 23rd International Electric Propulsion Conference, IEPC Paper 93-076, Sept. 1993.
[25]Belan, N. V., Kim, V., Oranstky, A. I., and Tikhonov, V. B., *Stationary Plasma Thrusters*, KHAI, Kharkov, Ukraine, 1989, p. 985 (in Russian).
[26]Rudolph, L. K., "The MPD Thruster Onset Current Performance Limitation," Ph.D. Dissertation, Princeton Univ., Princeton, NJ, 1981.
[27]Cory, J. S., "Mass, Momentum and Energy Flow from an MPD Accelerator," Ph.D. Dissertation, Princeton Univ., Princeton, NJ, 1971.
[28]Saber, A. J., "Anode Power in a Quasi-Steady MPD Thruster," Ph.D. Dissertation, Princeton Univ., Princeton, NJ, 1974.
[29]Kaplan, D. I., "Performance Characteristics of Geometrically Scaled MPD Thrusters," M.S. Thesis, Princeton Univ., Princeton, NJ, 1982.
[30]Choueiri, E. Y., and Kelly, A. J., and Jahn, R. G., "MPD Thruster Instability Studies," AIAA Paper 87-1067, Sept. 1987.
[31]Choueiri, E. Y., "An Introduction to the Plasma Physics of the MPD Thruster," Princeton Univ., TR MAE 1776.33, Dec. 1991.
[32]Polk, J. E., Kelly, A. J., and Jahn, R. G., "Characterization of Cold Cathode Erosion Processes," AIAA Paper 88-075, Sept. 1988.
[33]Hoskins, W. A., "Asymmetric Discharge Patterns in the MPD Thruster," M.S. Thesis, Princeton Univ., Princeton, NJ, 1990.
[34]Diamant, K. D., Choueiri, E. Y., and Jahn, R. G., "The Role of Spot Mode Transition in the Anode Fall of Pulsed MPD Thrusters," 24th International Electric Propulsion Conf., IEPC Paper 95-234, Sept. 1995.
[35]Randolph, T. M., Von Jaskowsky, W. F., Kelly, A. J., and Jahn R. G., "Measurement of Ionization Levels in the Interelectrode Region of an MPD Thruster," AIAA Paper 92-3460, July 1992.
[36]Choueiri, E. Y., and Okuda, H., "Anomalous Ionization in the MPD Thruster," 23rd International Electric Propulsion Conference, IEPC Paper 93-067, Sept. 1993.
[37]Choueiri, E. Y., Kelly, A. J., and Jahn, R. G., "Current-Driven Plasma Acceleration Versus Current-Driven Energy Dissipation Part II: Electromagnetic Wave Stability Theory and Experiments," 22nd International Electric Propulsion Conference, IEPC Paper 91-100, Sept. 1991.
[38]Tilley, D. L., Choueiri, E. Y., Kelly, A. J., and Jahn, R. G., "Microinstabilities in a 10-kW Self-field Magnetoplasmadynamic Thruster," *Journal of Propulsion and Power*, Vol. 12, No. 2, 1996, pp. 381–389.